HULL DETECTION BASED ON LARGEST EMPTY SECTOR ANGLE WITH APPLICATION TO ANALYSIS OF REALTIME MR IMAGES

Naveen Kumar, Shrikanth S. Narayanan

Signal Analysis and Interpretation Analysis Lab (SAIL)
Department of Electrical Engineering,
University of Southern California, Los Angeles, CA 90089
komathnk@usc.edu,shri@sipi.usc.edu

ABSTRACT

We present a novel view of the hull detection problem in two dimensions. Our proposed method is based on the principle of finding Pareto optimal boundaries and extends it to the general problem of finding a hull for a given set of points. We first compute the largest empty sector angle (LESA) score for each point. The desired hull can then be obtained as a super-level set of this score. We show how the proposed representation is related to a convex hull and demonstrate the flexibility it provides in choosing the geometry of the hull. As a target application we also present a head movement correction technique for real-time MR images of the dynamic vocal tract.

Index Terms— 2D hull detection, exterior point, convex hull, largest empty sector angle, MR image analysis

1. INTRODUCTION

The problem of hull detection for a set of points $\mathbf{X} = \{x_1, x_2, \ldots, x_n\}$ is defined as finding a subset $\mathbf{H} \subseteq \mathbf{X}$ of these points, such that the the polygon defined by the points in $\mathbf{H}$ contains all the points in $\mathbf{X}$. Different algorithms for hull detection can be categorized by the criteria they impose on the hull. For example, convex hull detection algorithms [1, 2, 3, 4, 5] popular in mathematics and computational geometry, require that $\mathbf{H}$ be the smallest convex set of points such that all points in $\mathbf{X}$ are contained in its convex hull. Convex hulls are preferred for their robustness in applications where precise boundary contours are not required [6, 7].

Although convex hulls for a given set of points can be computed in worst-case $O(nlog\ n)$ time [8] they might not suitable for certain other tasks. For example, in contour based shape matching the detected boundaries need to closely resemble the original shape of the object [9]. Non-convex hull detection algorithms [10, 11] have been proposed to find the "footprint" or area covered by a set of points in this case. These algorithms extend the Jarvis' March or gift-wrapping method [1] used for convex hull finding.

Several techniques have also been previously suggested for the task of boundary detection from images. In [12] the authors proposed to use statistical shape models to ensure smoothness in the object boundaries. Active contours or snakes [13] pose the problem as an energy minimization task, where external energy results from incorrect alignment of the contours and internal energy depends on its conformation. Weighting the internal energy lower makes the contours more deformable such that it fits the edges and lines better, while a higher internal energy acts as a smoothness constraint. The technique proposed in this paper, instead of directly finding an exact hull, computes an intermediate representation which can then be used to generate a hull with the desired geometry. We generalize the notion of a Pareto optimal frontier popular in the field of multi-objective optimization to find the boundary points of $\mathbf{X}$.

Specifically, for each point in $\mathbf{X}$ we find the angles corresponding to the largest empty sector (LESA) around that point. We denote this angle for each point x as $\delta(x)$. The intuition here is that for points lying on the boundary of $\mathbf{X}$, $\delta(x)$ should be larger compared to points in the interior and would ideally correspond to the exterior angles of the required hull. We illustrate properties of the super-level set $\mathbf{H}_\theta = \{x|\delta(x) \geq \theta, x \in \mathbf{X}\}$ and show that the proposed representation is directly related to convex hulls. By choosing different super-level sets $\mathbf{H}_\theta$ we can directly control the convexity of the generated hull. We show that the convex hull is obtained for the $\theta = 180^\circ$ super-level set, while choosing larger values of θ allows us to choose sharp points of interest on the boundary. As a target application, the proposed method is applied to real-time MR images of the human vocal tract [14] where they are used to detect sharp points on the silhouette of the face. This is used to track the position of the nosetip and chin in each frame, which can be in turn used to estimate and correct for any head movements in the data.

The algorithm for finding the largest empty sector angle is presented in Section 2. Section 3 establishes the relation between the proposed representation and finding Pareto optimal solutions and shows that the latter is special case. In Section 4 we discuss about the geometry of different super-level sets of $\delta(x)$ through examples. Relation of the proposed

representation with convex hulls is established. In Section 5 we present an application of the proposed representation for head movement correction in real time MR images. A brief summary of the proposed techniques and future directions are finally presented in Section 6.

2. FINDING THE LARGEST EMPTY SECTOR ANGLE

As a measure of whether a point lies on the boundary of a given set of points $\mathbf{X}$, we propose the following metric. We find the largest angular gap around each point which does not contain any of the other points (Fig. 1). The intuition is that points on the boundary will have larger empty sectors compared to the points in the interior. In this section, we describe the algorithm to find the largest empty sector angle (LESA) around each point. In the next section, we show how finding Pareto optimal points is a special case of this idea.

Without loss of generality let us assume that the origin is shifted to the current point of interest x_k i.e. $\mathbf{Y} = \{x_1 - x_k, x_2 - x_k, \ldots, x_{n-1} - x_k\}$. Further, let θ_i be the angle each point y_i subtends on the positive half of the x-axis measured in the counter-clockwise direction. Then the problem of finding the LESA, is equivalent to solving the problem

$$\begin{aligned} \max_{\alpha,\beta} \quad & \delta = |\alpha - \beta| \\ \text{s.t.} \quad & (\theta_i - \alpha)(\theta_i - \beta) \geq 0, \forall i = 1 \ldots n-1 \end{aligned} \tag{1}$$

where the angles α, β define the position of the largest empty sector.

It can be proved by contradiction that the optimal $\alpha^*, \beta^* \in \{\theta_1, \ldots, \theta_n\}$. This restricts the search space allowing the use of an efficient algorithm to find the solutions. The algorithm is described below in Algorithm 1.

Input: Set of points $\mathbf{Y} = \{y_1, \ldots, y_{n-1}\}$
Output: The largest empty sector angle δ about the origin

1: Compute the counter-clockwise angle subtended by each point in $\mathbf{Y}$ on the x-axis.
2: Sort the angles in ascending order as $\theta_1, \ldots \theta_{n-1}$
3: Calculate their first order difference $\phi_i = \theta_{i+1} - \theta_i$ for $i = 1, \ldots, n-2$
4: $\delta = \max_{i=1}^{n-2} \phi_i$

Algorithm 1: An algorithm for estimating the largest empty sector angle (δ)

Fig.2 shows an illustrative example of the LESA δ scores for a set of points. These points were detected by using the Canny edge detection algorithm on an MR image of the vocal tract. The obtained δ scores match the intuition that the exterior points have a higher score compared to the points in the interior. Moreover, points at the "corners" of the hull have the highest LESA scores. These MR images are formally introduced later in Section 5 when we propose an application for the analysis of realtime MRI sequences. Hence, we use this image as a running example throughout this paper.

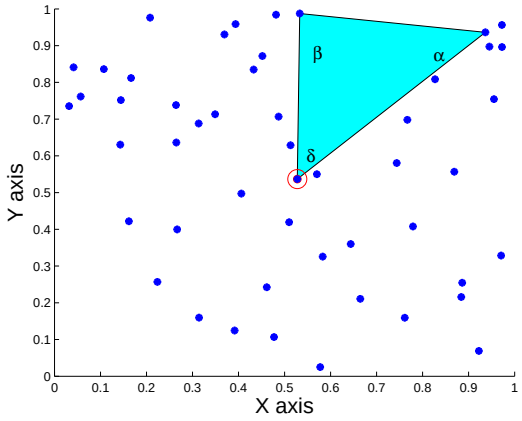

Fig. 1. The largest empty sector (shaded cyan) for one of the points (in the red circle) corresponding to the given set of points. The largest empty sector is bounded by angles α, β and subtends angle δ on the point.

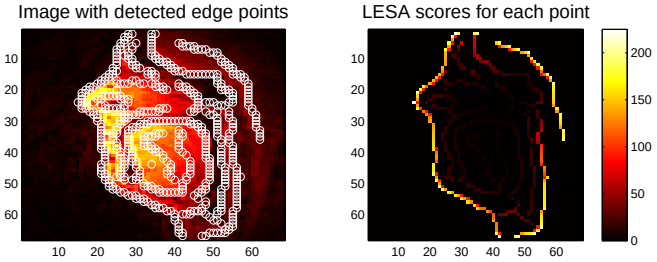

Fig. 2. Figure on the left shows the points detected by the Canny edge detector [15]. Right figure shows the LESA (δ) scores for the points. The LESA scores are higher for points on the exterior.

3. RELATION TO PARETO OPTIMAL BOUNDARIES

In this section, we show how finding the Pareto optimal boundary for a given set of points can be considered to be a special case of the empty sector angle representation described above. The notion of Pareto efficiency is useful in multi-objective optimization problems where it helps select candidate solutions at the boundary of a tradeoff / ROC curve. Specifically, for two objective functions $f(t), g(t)$ for a solution t, that are being traded off against each other, according to Pareto efficiency, a solution t_1 is said to be more efficient than t_2 iff, $f(t_1) < f(t_2)$ and $g(t_1) < g(t_2)$. This minimal notion of efficiency then allows us to define Pareto optimal points as follows.

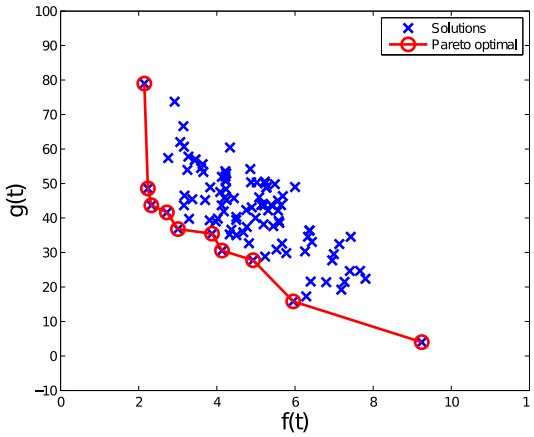

Fig. 3. Pareto optimal solutions for a multi-objective minimization problem. Blue crosses indicate candidate solutions for the optimization problem.

Definition 1. *A solution t is Pareto optimal for objective functions f, g iff $\nexists s \;\; s.t. \; f(s) < f(t), g(s) < g(t)$*

Fig.3 illustrates Pareto optimality in the context of a dual objective minimization problem. Note that the set of pareto-optimal points gives their "left-bottom" boundary. Geometrically, it means that a solution that is Pareto-optimal for a dual objective minimization problem, must have an empty third quadrant when the origin is shifted to that point. Note, that if we change each optimization problem to maximization/ minimization we alter the geometric requirement to other quadrants and can find extremal points in other directions. Each of these four optimization problems can be viewed as special cases of finding the points with largest empty sector angle $\delta \geq 90°$ and $\alpha = 0°, 90°, 180°, 270°$. Computing the LESA δ for each point in $\mathbf{X}$ allows us to generalize the problem with respect to the angle and orientation of the sectors, thereby providing a control on the shape of hull boundary.

4. GEOMETRY OF THE HULL

In the previous section we established the relation between LESA scores and Pareto optimal points. In this section we examine how LESA scores can be used to control the geometry of the hull. To better interpret the LESA scores, in Fig.4 we show the hulls obtained by the super-level sets $\mathbf{H}_\theta$ for different angles θ. Note that the hull obtained by thresholding $\delta \geq 180°$ closely resembles its convex hull. It can be in fact shown that $\mathbf{H}_\pi = \{x \mid \delta(x) \geq 180°, x \in \mathbf{X}\}$ is the convex hull by use of the supporting hyperplane theorem which states that if $\mathbf{S}$ is a closed set with non-empty interior such that for each point x_0 on its boundary there exists a supporting hyperplane, then $\mathbf{S}$ is a convex set.

$\delta(x) \geq 180°$ is equivalent to the statement that a supporting hyperplane/ tangent exists at that point x. This ensures that the set $\mathbf{H}_\pi$ is convex. Additionally, we observe that $\mathbf{H}_\pi$ corresponds to the smallest such convex set making it the convex hull.

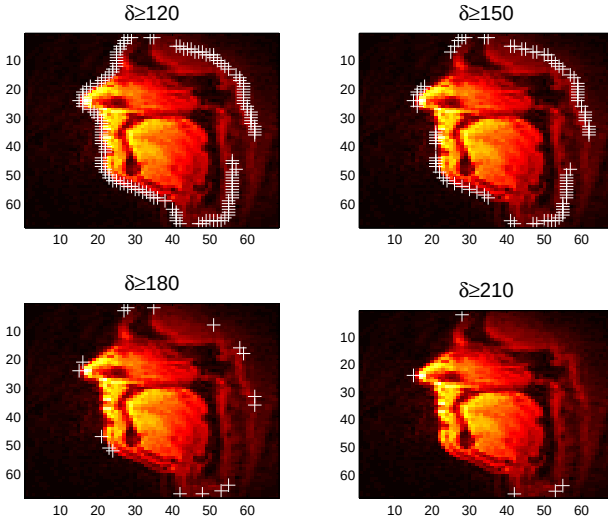

Fig. 4. The super-level sets obtained for different thresholds. Note $\delta \geq 180°$ gives a convex hull. For thresholds$> 180°$ the polygon does not enclose all the points.

As the value of the threshold θ is decreased below $180°$ the resulting hull is increasingly concave, as can be seen by the inclusion of the nose bridge in the MR image while going from $\delta \geq 150°$ to $\delta \geq 120°$. A higher threshold on δ on the other hand highlights the corners and sharper points on the boundary which is an important problem in many tasks.

In this paper, we apply the proposed hull detection approach to the analysis of real time magnetic resonance images. In particular, using the landmark detection afforded by this proposed method, we perform head motion correction in the acquired image sequences as described in the next section.

5. HEAD MOVEMENT TRACKING AND CORRECTION IN REAL-TIME MR IMAGE SEQUENCES

Real-time Magnetic Resonance Imaging (rtMRI) [16] captures the moving vocal tract during speech production and swallowing activities and hence serves as an invaluable tool for researchers studying speech production and other clinical applications such as swallowing disorders. The hull detection proposed in this paper can be useful in analyzing the MRI sequences.

One of the key problems is the subject's head motion during image acquisition that renders subsequent analyses difficult. Generally there are no fiducial reference markers available for this purpose, and hence reliance on anatomical landmarks is common. We describe a reference point (landmark) based head motion correction technique. The target landmarks are the nosetip and chin for this purpose. We use the δ

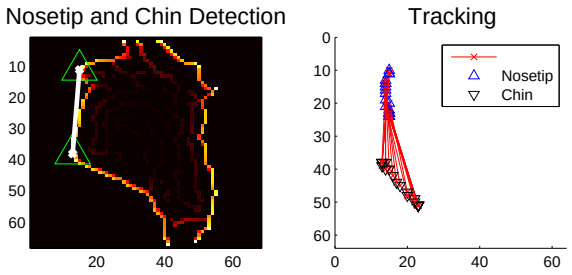

Fig. 5. Nosetip and chin detection and tracking

scores for locating the position of nosetip and chin in the MR image. These two points are then tracked over time, to obtain an estimation of the rotation and translation for each frame.

As shown in Fig.4 higher values of δ typically correspond to larger exterior angles and hence sharp points on the boundary. Since the nosetip and chin are two sharp features on the boundary, this fact can be exploited to locate their position in these MR images (Fig.5). Our method is similar to the convex hull based finger-tip tracking technique proposed in [6, 7]. However, instead of convex hulls we use the proposed LESA representation which allows us to fit a custom hull (Fig. 6) suited for this purpose which allows to robustly locate the landmark points. The approach is summarized in Algorithm 2.

Input: LESA scores δ for all edge points $x_1, \ldots, x_n$
Output: Position of the nosetip $n(t)$ and chin $c(t)$ at time t

1: Only retain the sharp points for which $\delta \geq \delta_{th}$. Suppose there are k remaining points.
2: Compute the center $\overline{x_{sh}}$ for the remaining points
3: Sort the points $x_1, \ldots, x_k$ according to the angle subtended by $(x_1 - \overline{x_{sh}})$ in a counterclockwise direction.
4: $n(t) \leftarrow x_1$
5: $c(t) \leftarrow x_k$

Algorithm 2: Algorithm for detecting nosetip and chin in rtMRI images

The nosetip and chin detection scheme is illustrated in Fig.6. For our experiments a threshold value of $\delta_{th} = 195^\circ$ was used in Algorithm 2.

The rotation and translation are estimated by assuming the nosetip to be the center of rotation. All subsequent frames are rotated and aligned with respect to the first frame. To correct the movement in a frame it is first shifted such that the nosetips are aligned. Then the image is rotated about the nosetip by the estimated angle of rotation. Fig.7 shows a sample head motion corrected frame.

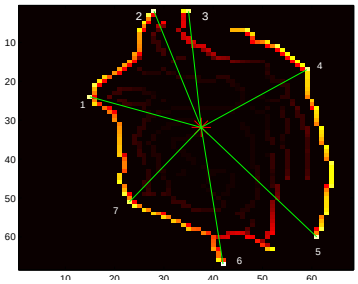

Fig. 6. Selecting the nosetip and chin position by ordering the "sharp" points in a counter-clockwise fashion. Number next to each vertex indicates the sorting index.

6. CONCLUSION

We presented a largest empty sector angle (LESA) representation for a set of points which can be used to generate a hull with desired geometry. We show that the convexity of the generated hull can be parametrized by choosing the appropriate super-level set $\mathbf{H}_\theta$. In the special case $\theta = 180^\circ$ a convex hull is obtained. For larger θ, $\mathbf{H}_\theta$ comprises of sharp points on the boundary of $\mathbf{X}$. We apply this method for the analysis of realtime MR image (rtMRI) sequences. In particular we focus on the problem of tracking and correcting for head movement during image acquisitions. Specifically, we exploit the ability of the proposed algorithm to detect sharp points for finding the nosetip and chin in rtMRI images and propose a technique for robust head movement correction.

Future work should consider extending this method for hull finding in higher dimensions. Additionally, an extension to grayscale 2D images might allow us to do away with the initial segmentation stage. Finally, we would also like to evaluate the proposed method on contour based shape matching applications by allowing for custom degrees of convexity in the hull finding.

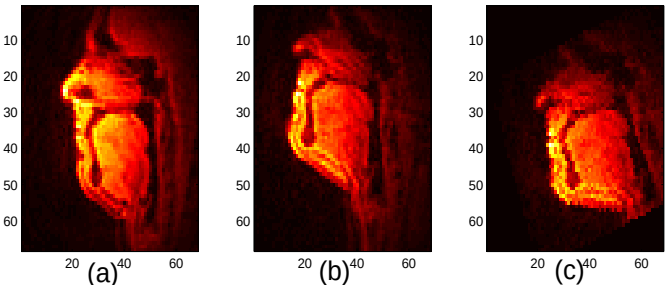

Fig. 7. a) The first frame b) The current image frame showing head movement c) Current image frame motion corrected to align with the first frame

7. REFERENCES

[1] Ray A Jarvis, "On the identification of the convex hull of a finite set of points in the plane," *Information Processing Letters*, vol. 2, no. 1, pp. 18–21, 1973.

[2] Ronald L. Graham, "An efficient algorith for determining the convex hull of a finite planar set," *Information processing letters*, vol. 1, no. 4, pp. 132–133, 1972.

[3] Timothy M Chan, "Optimal output-sensitive convex hull algorithms in two and three dimensions," *Discrete & Computational Geometry*, vol. 16, no. 4, pp. 361–368, 1996.

[4] Alex Bykat, "Convex hull of a finite set of points in two dimensions," *Information Processing Letters*, vol. 7, no. 6, pp. 296–298, 1978.

[5] C Bradford Barber, David P Dobkin, and Hannu Huhdanpaa, "The quickhull algorithm for convex hulls," *ACM Transactions on Mathematical Software (TOMS)*, vol. 22, no. 4, pp. 469–483, 1996.

[6] Xiao-Heng Jiang, Jiang-Wei Li, Kong-Qiao Wang, and Yan-Wei Pang, "A robust method of fingertip detection in complex background," *Internation Conference of Machine Learning and Cybernetics,2012*.

[7] S Nagarajan, TS Subashini, and V Ramalingam, "Vision based real time finger counter for hand gesture recognition," *CPMR- International Journal of Technology*.

[8] Andrew Chi-Chih Yao, "A lower bound to finding convex hulls," *Journal of the ACM (JACM)*, vol. 28, no. 4, pp. 780–787, 1981.

[9] Dengsheng Zhang and Guojun Lu, "Review of shape representation and description techniques," *Pattern recognition*, vol. 37, no. 1, pp. 1–19, 2004.

[10] Antony Galton and Matt Duckham, "What is the region occupied by a set of points?," in *Geographic Information Science*, pp. 81–98. Springer, 2006.

[11] Adriano Moreira and Maribel Yasmina Santos, "Concave hull: A k-nearest neighbours approach for the computation of the region occupied by a set of points," 2007.

[12] Yongmei Wang and Lawrence H Staib, "Boundary finding with correspondence using statistical shape models," in *Computer Vision and Pattern Recognition, 1998. Proceedings. 1998 IEEE Computer Society Conference on*. IEEE, 1998, pp. 338–345.

[13] Timothy F Cootes and Christopher J Taylor, "Active shape modelssmart snakes," in *BMVC92*, pp. 266–275. Springer, 1992.

[14] Shrikanth Narayanan, Erik Bresch, Prasanta Kumar Ghosh, Louis Goldstein, Athanasios Katsamanis, Yoon Kim, Adam C Lammert, Michael I Proctor, Vikram Ramanarayanan, and Yinghua Zhu, "A multimodal real-time mri articulatory corpus for speech research.," in *INTERSPEECH*, 2011, pp. 837–840.

[15] John Canny, "A computational approach to edge detection," *Pattern Analysis and Machine Intelligence, IEEE Transactions on*, , no. 6, pp. 679–698, 1986.

[16] Shrikanth Narayanan, Krishna Nayak, Sungbok Lee, Abhinav Sethy, and Dani Byrd, "An approach to real-time magnetic resonance imaging for speech production," *The Journal of the Acoustical Society of America*, vol. 115, pp. 1771, 2004.